Evaluation of Topologies and Active Control Methods for Overvoltage Mitigation in SiC-Based Motor Drives

Mohamed S. Diab, Wenzhi Zhou, and Xibo Yuan
Department of Electrical and Electronic Engineering
University of Bristol
Bristol, United Kingdom
mohamed.diab@bristol.ac.uk, wenzhi.zhou@bristol.ac.uk, xibo.yuan@bristol.ac.uk

***Abstract*—Silicon-carbide (SiC) based power converters are gaining momentum as a genuine alternative to silicon based counterparts for motor drive applications that require high efficiency, power density, and operating temperatures. However, the motor terminal overvoltage due to the reflected voltage phenomenon across power cables is more pronounced in SiC-based drives due to the fast-switching speeds of SiC power devices. Since the resultant overvoltage has severe effects on motor winding insulation, several approaches have been developed to mitigate the motor terminal overvoltage including passive filtering techniques and active control methods. With passive filters being widely assessed and reviewed, this paper evaluates the effectiveness of the active control methods, including multilevel converters, soft-switching techniques, and modified PWM schemes, in a qualitative and quantitative comparative study. The active control methods, along with the adopted power converter topologies, are assessed considering their effectiveness in motor terminal overvoltage mitigation, component count and rating, power loss, reliability, and pros and cons. Experimental results based on a three-phase 7.5kW induction motor are provided to support the comparative study.**

***Keywords*—High *dv/dt*, inverter-fed motors, motor overvoltage, reflected voltage phenomenon, silicon carbide (SiC).**

I. Introduction

The emergence of silicon carbide (SiC) power devices enables motor drives to achieve a better performance, compared to those based on traditional silicon (Si) power devices, due to the superior characteristics of SiC material. The fast-switching speeds and elevated temperature capabilities of SiC devices allow motor drives to operate at high switching frequencies and reduced cooling requirement, which results in enhanced efficiency and power density [1]. However, the high voltage slew-rate (dv/dt) associated with the fast-switching transitions of SiC devices results in voltage reflections across the power cables that connect the inverter cabinet and the motor unit. This returns to the impedance mismatch between the cable and the motor, where the PWM voltage pulses experience back and forth voltage reflections between the inverter and the motor resulting in high-frequency overvoltage oscillations at the motor terminals [2]-[4]. These oscillations increase the stresses on the motor where depending on the drive system characteristics, they can damage the stator winding insulation either in the short or long term [5].

Several parameters can affect the peak motor overvoltage due to the reflected voltage phenomenon. These parameters are the motor and cable impedance, the pulse rise time, and the wave propagation time which depends on the cable length. When the motor impedance is significantly higher than the cable impedance, the voltage pulses travelling from the inverter to the motor across the power cables can experience full voltage reflection. Depending on the cable length, the motor voltage can be twice the inverter voltage (known as doubled voltage effect). The minimum cable length at which the doubled voltage effect occurs is denoted as the critical length which is directly proportional to the pulse rise time [6]. That is, as the pulse rise time shortens, the critical cable length decreases. This is demonstrated in Fig. 1, where the motor overvoltage is sketched versus the cable length at different rise times (t_r) [7]. It can be noticed that the advantageous shorter switching times of SiC power devices, which can be as little as tens of nanoseconds, can stimulate the doubled voltage effect in SiC-based motor drives at shorter cable lengths (e.g., within few meters), compared to Si-based counterparts.

Several approaches have been introduced in literature to mitigate the motor overvoltage due to the reflected voltage phenomenon. These approaches can be classified into passive and active techniques. The passive techniques adopt various filter networks either at the inverter side, motor side, or both sides to suppress the overvoltage transients at the motor terminals. Different passive filter designs have been developed

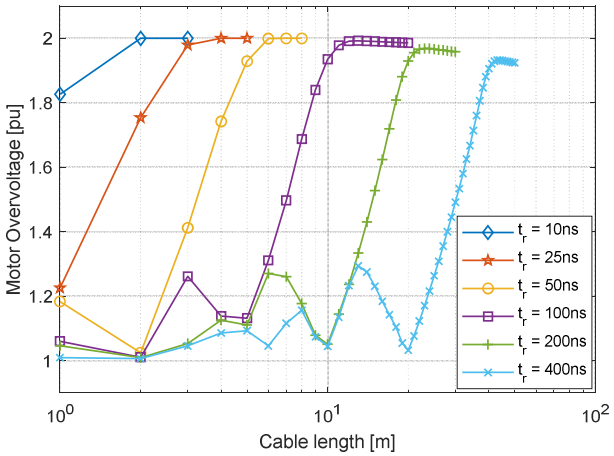

Fig. 1 Overvoltage variation in relation to cable length and pulse rise time.

and investigated in various studies under two categories: dv/dt filters and impedance matching filters. The dv/dt filters reduce the overvoltage transients by limiting the voltage derivative applied to the system. Whereas, the impedance matching filters alleviate the impedance difference between the cable and motor. The passive filtering techniques have been widely reviewed in several articles [8]-[11] showing that they can satisfactorily mitigate the motor overvoltage, however, with additional power loss, size, and cost to the drive system. Moreover, some filter networks are specifically designed for a certain cable length, where the variation of the cable length requires re-designing the filter parameters.

Eradicating inverter-/motor-side filters, active control methods have been adopted to mitigate the motor overvoltage based on modified PWM schemes, soft-switching techniques, and multilevel converter topologies. This paper reviews these active control methods highlighting their operation principles and effectiveness in overvoltage mitigation with experimental demonstration on three SiC converter topologies to provide a like-for-like comparison for the first time.

II. Fundamentals of Voltage Reflection

The two-level (2L) voltage-source inverter, shown in Fig. 2, is the most common inverter topology used in industrial drives to control electric motors in a wide-speed range, where the sinusoidal PWM technique is often utilized to generate the driving signals of the employed switching devices. In some industrial applications (such as submersible and high ambient temperature applications), the motor should be separately placed from the inverter where power cables are used for interconnection. Similar to travelling waves in transmission lines, the PWM voltage pulses experience back and forth reflections across the cables resulting in overvoltage oscillations at the motor terminals. The relationship between the motor peak voltage (V_m) and the inverter voltage (V_s) is expressed as [9]:

$$V_m = (1 + \Gamma_{\mathrm{m}})\, V_s, \ \text{for } t_{\mathrm{r}} \ll 3t_p \tag{1a}$$

$$V_m = \left(1 + \frac{3t_p}{t_r}\Gamma_{\mathrm{m}}\right) V_s, \ \text{for } t_{\mathrm{r}} \gg 3t_p \tag{1b}$$

where t_r is the pulse rise time, t_p is the wave propagation time across the cable, and Γ_{m} is the motor reflection coefficient. Since the motor impedance is always several times higher than that of the cable, the motor appears as an open circuit to the voltage surge travelling across the cable, where Γ_{m} is reasonably approximated to unity [9]. Thus, based on (1a), when the pulse rise time is significantly shorter than triple the wave propagation time, the motor voltage can be twice the inverter voltage. With fast-switching speeds of SiC devices, the doubled voltage effect can be stimulated at shorter cable lengths than used when Si devices are adopted.

The motor terminal overvoltage in 2L-inverter-fed drives is experimentally demonstrated using a three-phase SiC inverter based on Wolfspeed C2M0040120D SiC MOSFETs. The inverter supplies a three-phase 7.5kW motor through 12.5-m long four-core 13 AWG PVC cable, as shown in Fig. 3. The inverter is supplied from 500V dc-link and is switched at 20kHz. The SiC MOSFETs are triggered through gate drivers

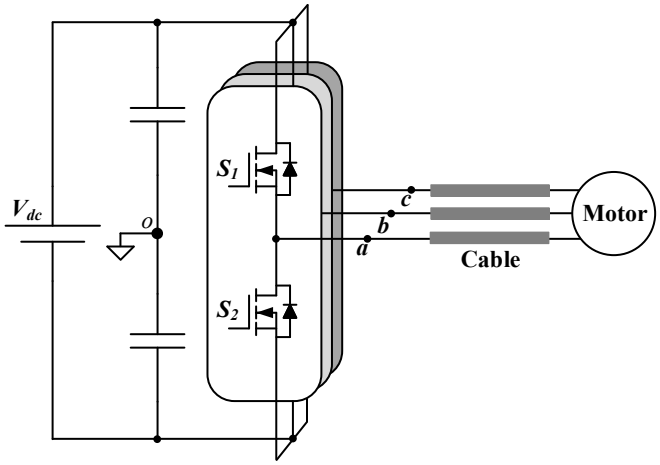

Fig. 2 Circuit diagram of 2L voltage-source inverter supplying a three-phase motor through power cables.

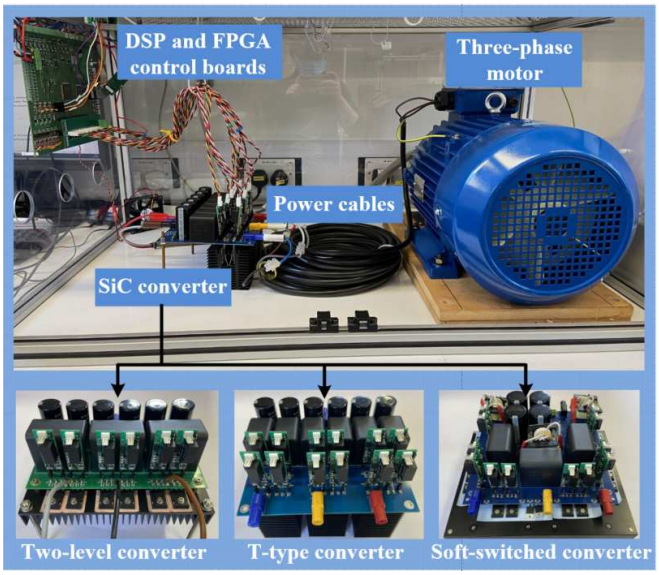

Fig. 3 Hardware view of experimental setup including three different SiC converter topologies.

with 25Ω gate resistance where the switching rise/fall time of the PWM voltage pulses is 50ns. The wave propagation time, based on the connected cable length, is 80ns. Since the pulse rise time is significantly lower than triple the wave propagation time, the PWM voltage pulses can experience doubled voltage effect, as indicated by (1a). This is experimentally illustrated in Fig. 4, where the motor peak voltage is double the inverter voltage with transient oscillations at both rising and falling voltage transitions. The doubled motor voltage increases the possibility of partial discharge (PD) inception within the winding turns, which can result in premature failure of winding insulation.

III. Active Control Methods for Overvoltage Mitigation

Different approaches have been used as filter-less solutions to mitigate the motor overvoltage in SiC-based PWM drives. These approaches are addressed and evaluated in the following subsections.

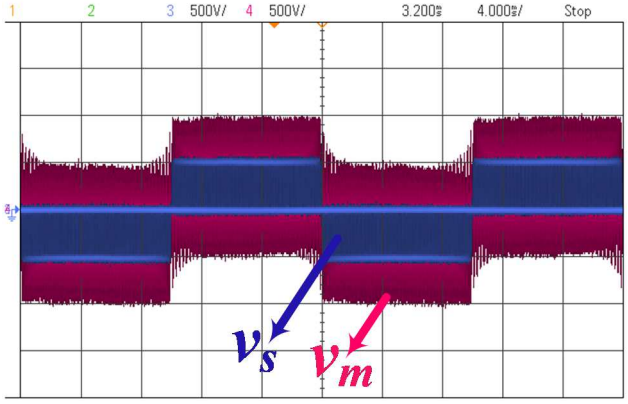

(a)

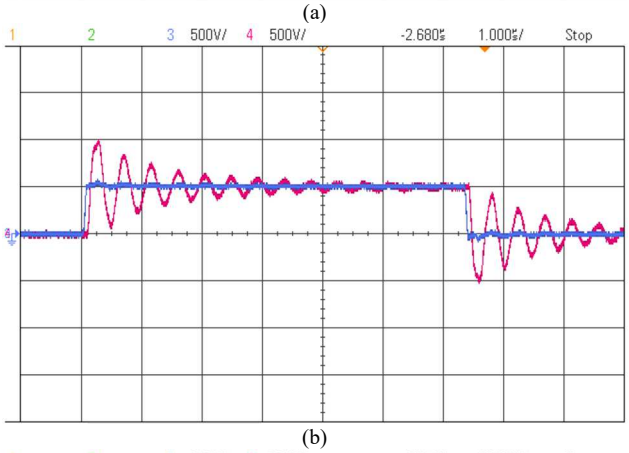

(b)

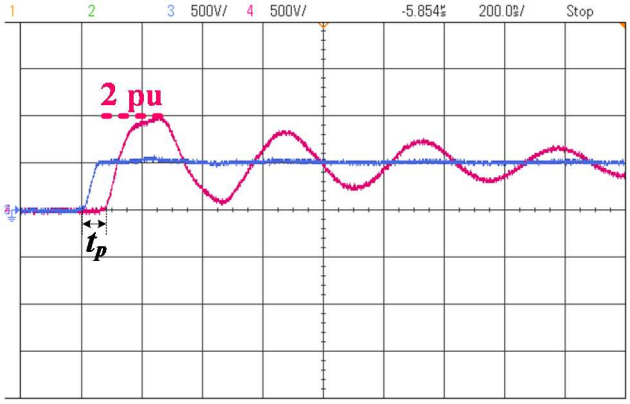

(c)

Fig. 4 Experimental demonstration of voltage reflection phenomenon in a 2L inverter: (a) inverter and motor voltages along with load currents, (b) switching cycle view, and (c) enlarged view for a rising voltage transition.

A. Multilevel Converter Topologies

Multilevel converters are able to generate PWM voltage pulses synthesized in multilevel, resembling a sinusoidal waveform. As the number of levels increases, the inverter output voltage clearly resembles sinusoidal curvature with minimal harmonic contents [12]. However, this comes at the expense of employing increased component count incurring additional size, cost, and power loss, which can be justified for medium-voltage motor drives [13]. For low-voltage motor drives, three-level (3L) converters can be used as feasible replacement for 2L converters with enhanced efficiency. The T-type converter, shown in Fig. 5, is a simple example that can be used to generate 3L voltage waveform. It inherits the structure of standard 2L converters, however, with auxiliary

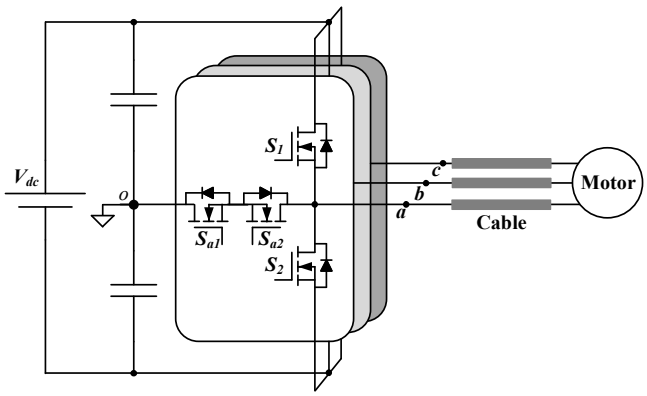

Fig. 5 Circuit diagram of T-type converter supplying a three-phase motor through power cables.

branches connecting the dc-link midpoint to the output nodes of each phase leg. The auxiliary branches are realized using a bidirectional switch that is commonly implemented via a pair of switching devices in common-source configuration. Since the bidirectional switch only needs to block half of the dc-link voltage, the auxiliary switching devices are rated at $0.5V_{dc}$. The modulation, control, and commutation process of the T-type converter are detailed in [14]. Compared with the 2L converter, the switching loss of the T-type converter is lower due to the halved commutation-voltage across the switches, whereas the conduction loss does not considerably change [15].

When the 3L T-type converter is used in cable-fed motor drives, the output voltage still experiences voltage reflection since the voltage waveform is pulse modulated. However, the peak motor voltage is quantified by the overvoltage associated with the highest voltage level during the modulation cycle, where other lower voltage levels experience overvoltage that is always lower than V_{dc} (i.e., lower than the inverter rated voltage). This is experimentally illustrated in Fig. 6, where a 3L T-type converter is used as a cable-fed motor drive with the same experimental parameters used in the 2L converter case study. It can be noticed that the inverter output line voltage has five voltage levels between the two pole voltages. Importantly, the motor experiences terminal overvoltage oscillations, due to the cable effect, with a peak voltage limited to 1.5 times the inverter rated voltage (i.e., the peak motor voltage is 1.5 pu at most). Compared with the 2L converter, the 3L converter reduces the motor overvoltage by 50%, which in turn reduces the PD likelihood in motor winding insulation. This is because the voltage change (ΔV) of the 3L waveform is half of that in the 2L waveform.

B. Modified PWM Patterns

Instead of using 2L and 3L modulation schemes, a quasi-three-level (Q3L) modulation strategy has been suggested to mitigate the motor overvoltage in cable-fed motor drives [16], [17]. The key idea of the Q3L approach is reshaping the PWM voltage transition pattern based on the observation that the voltage reflection across the connection cables can be cancelled by splitting the rising and falling transitions of the 2L PWM voltage pulses into two identical voltage steps with an appropriate separation time. In the midst of the split voltage transition, an intermediate voltage level is temporarily adopted, as elucidated in Fig. 7. Since the resultant voltage pulses have an interim voltage level in the transition

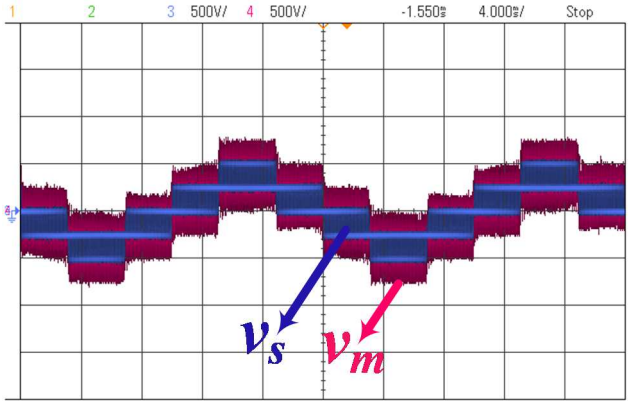

(a)

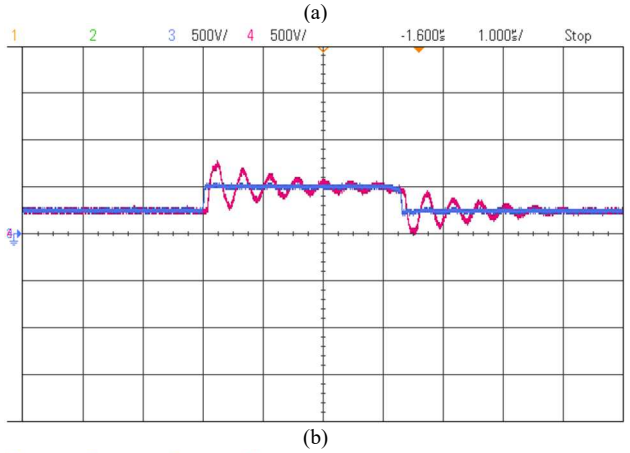

(b)

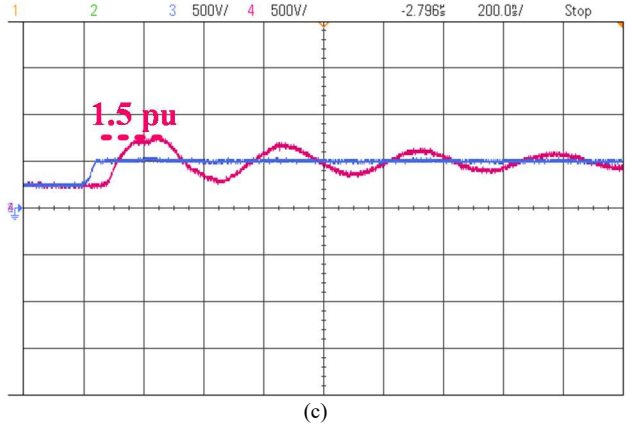

(c)

Fig. 6 Experimental demonstration of voltage reflection phenomenon in a 3L T-type inverter: (a) inverter and motor voltages along with load currents, (b) switching cycle view, and (c) enlarged view for a rising voltage transition.

between the two pole voltages, the modulation scheme is denoted as Q3L PWM. The delay time separating the two switched voltage steps is referred to as the dwell time t_d which depends on the wave propagation time t_p, as [16]:

$$t_d = 2t_p \tag{2}$$

The optimal setting of the dwell time, based on (2), allows the voltage reflection of the first voltage step to be significantly counterbalanced by the incidence of the second voltage step, as detailed in [17]. Depending on the reflection coefficients at the inverter and motor sides, it has been shown that the motor overvoltage can be limited to 20% at most [17].

The Q3L PWM technique can be implemented based on either unipolar modulation using the T-type converter [16] or

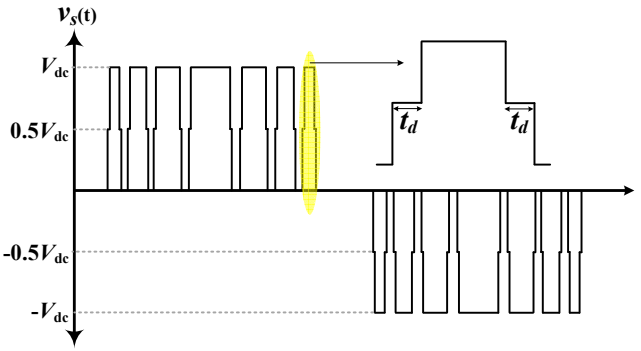

Fig. 7 Q3L approximation using unipolar modulation.

bipolar modulation using a dual voltage-source converter for open-winding motor drives [18]. In this paper, the T-type converter, shown in Fig. 5, is used for experimental evaluation of the Q3L PWM scheme, with the same experiment parameters previously used. Based on the connected cable length, the dwell time is 160ns. Fig. 8 shows the effectiveness of Q3L T-type converter in mitigating the reflected voltage phenomenon, where the peak motor voltage is 1.15 pu. The enlarged view (see Fig. 8c) shows that the motor voltage has a 2L waveform crossing the inverter Q3L waveform at the dwell time midway.

It should be noted that the switches in the auxiliary branch of the Q3L T-type converter only conduct during the intermediate voltage level which lasts for a brief time (the dwell time). Thus, the current rating and conduction loss of these switches are much lower than that of the main switches, unlike the case in a standard 3L T-type converter. Further, the switching devices in the auxiliary branches only block half of the dc-link voltage. Therefore, the switching devices of the auxiliary branches can be implemented with lower voltage and current rating. On the other side, the effectiveness of the Q3L PWM scheme depends on the setting accuracy of the dwell time which depends on the wave propagation time, as elucidated in (2). In many practical cases, it is difficult to obtain an accurate value of the wave propagation time where cable operating temperature may affect its insulation permittivity and thus change its electrical characteristics. Although the variation in the wave propagation time with operating temperature is not considerably high (e.g., within $\pm$10%), the consequent impact on the mitigation ability of the Q3L method should be highlighted.

C. Soft-Switching Techniques

Referring to (1b), when the rise time is significantly longer than triple the wave propagation time, the peak motor voltage can be maintained close to the inverter rated voltage (i.e., within safe limits). Traditionally, the switching rise/fall times can be lengthened by increasing the gate resistance of the employed gate driver. However, this increases the switching power loss of the converter and dispossesses the SiC power devices from their prominent advantage of fast-switching speeds. Alternatively, soft-switching techniques can be used to decouple the switched voltage and current such that the consequent switching power loss is near zero. This allows the switching rise/fall times be fairly controlled, using additional resonant elements, with minimal impact on the converter efficiency.

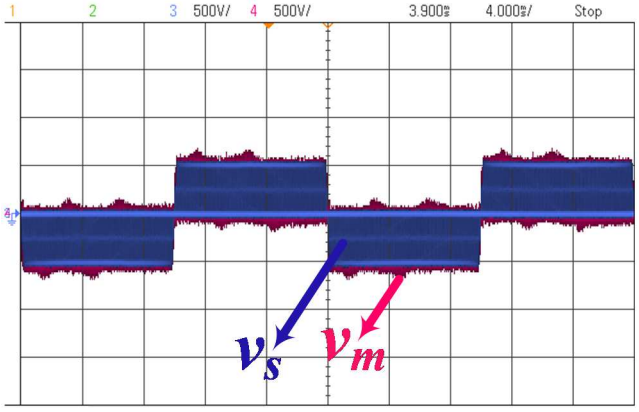

(a)

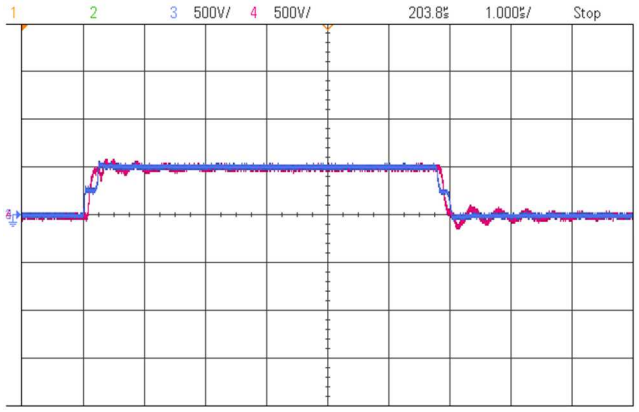

(b)

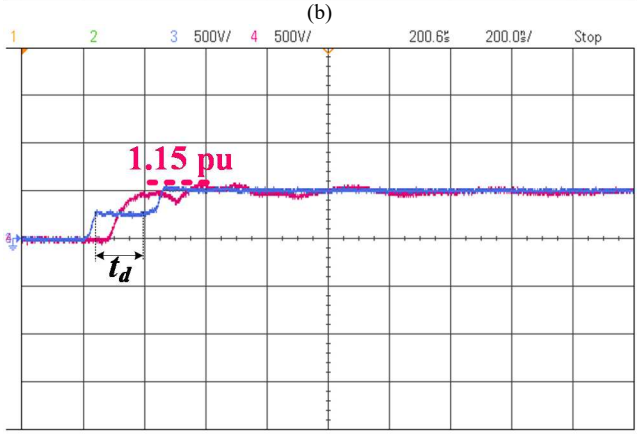

(c)

Fig. 8 Experimental demonstration of voltage reflection phenomenon in a Q3L T-type inverter: (a) inverter and motor voltages along with load currents, (b) switching cycle view, and (c) enlarged view for a rising voltage transition.

In [19], a soft-switching inverter, denoted as the auxiliary resonant commutated pole inverter (ARCPI), has been presented as an overvoltage mitigation tool for SiC-based motor drives. Its conceptual idea is based on profiling the voltage transitions with controllable dv/dt rate using a resonant circuit, without sacrificing the beneficial attributes of SiC switching devices. As shown in Fig. 9, each phase of the ARCPI involves a standard half-bridge circuit (S_1 and S_2) incorporated with an auxiliary resonant circuit between the phase-leg output node and the dc-bus middle point. The auxiliary resonant circuit is composed of two auxiliary switches (S_{a1} and S_{a2}), a resonant inductor (L_r), and two snubber capacitors (C_{r1} and C_{r2}). Through a resonance action between the resonant inductor and the snubber capacitors, the main

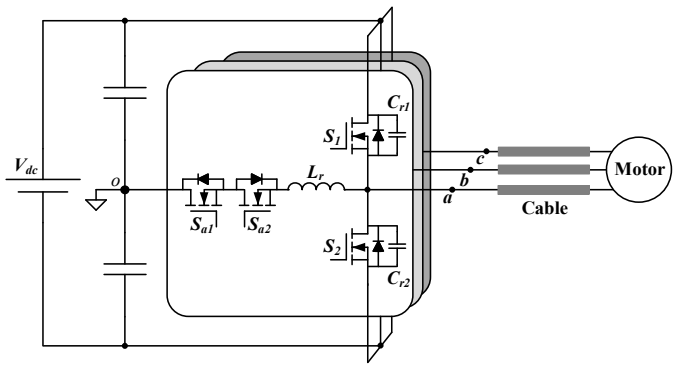

Fig. 9 Circuit diagram of auxiliary resonant commutated pole soft-switched inverter supplying a three-phase motor through power cables.

switches are turned ON/OFF under zero-voltage switching while the auxiliary switches are turned ON/OFF under zero-current switching [20]. This results in smoothed output voltage fronts, in a sinusoidal manner, with reduced switching power loss. The resonant inductance and snubber capacitance are designed based on the required switching rise time which is selected, depending on the cable length, to be much longer than triple the wave propagation time to eliminate the motor overvoltage. In addition to mitigating the motor overvoltage, the ARCPI attenuates the high-frequency electro-magnetic interference (EMI) since the output voltage edges are quietened [20].

Fig. 10 shows experimental results for the ARCPI operation with the same experimental parameters used before. With 2.7μH and 8.2nF resonance inductance and capacitance, respectively, the switching rise/fall time is 400ns; significantly longer than triple the wave propagation time (t_p = 80ns). This results in zero overvoltage at the motor side, where the motor voltage is almost coincided with the inverter voltage (i.e., the peak motor voltage is 1 pu).

IV. Assessment

Table I presents a summarized performance assessment for the reviewed active control methods for motor terminal overvoltage mitigation in SiC-based drives, with the 2L converter being used as a reference for comparison. The 3L T-type converter achieves 50% reduction in the motor terminal overvoltage since the output voltage waveform is synthesized in 3L rather than 2L, which results in halved voltage jump (dv/dt) and accordingly improved total harmonic distortion and EMI performance. Although the 3L T-type converter employs double the number of switching devices compared with the 2L converter, the supernumerary switching devices have a voltage rating that is half that of the main switching devices. Since the switching devices of the T-type converter operate at halved commutation voltage, compared with the 2L converter, the switching losses of the 3L T-type converter is lower than that of the 2L converter in the medium switching frequency range. Also, the conduction losses of the T-type converter does not change considerably compared with the 2L converter. Therefore, depending on the switching frequency, the efficiency of the 3L T-type converter can be higher than the efficiency of the 2L converter [15].

The Q3L T-type converter achieves further reduction in the motor terminal overvoltage, compared with the 3L T-type

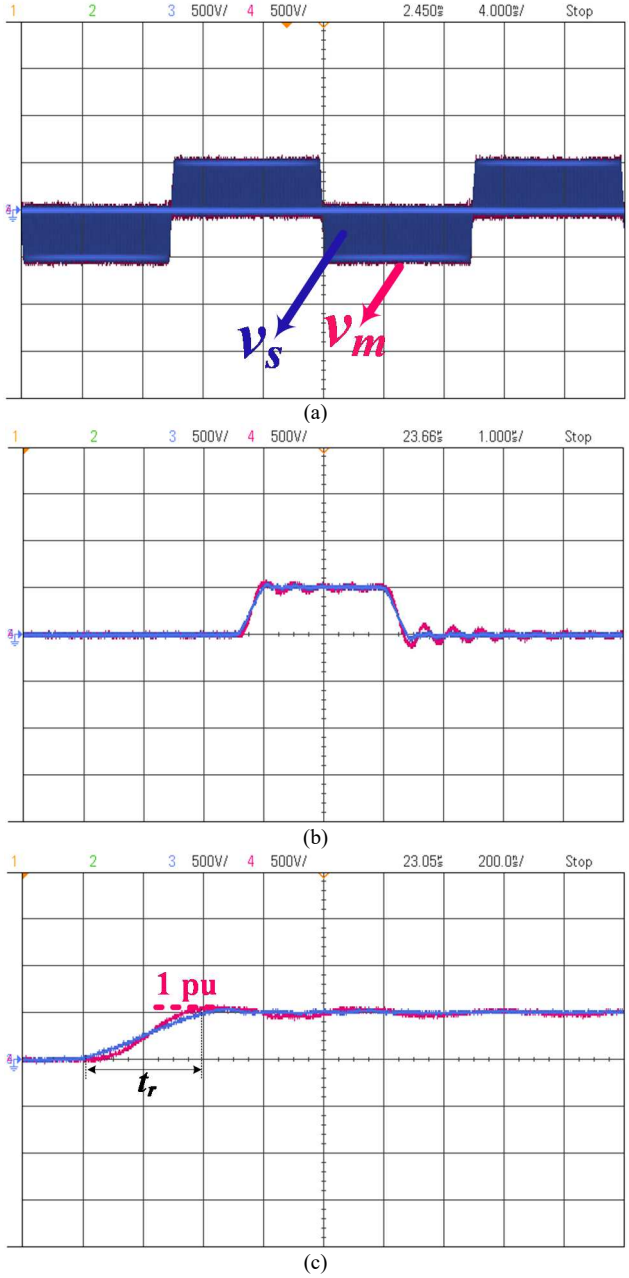

Fig. 10 Experimental demonstration of voltage reflection phenomenon in a soft-switched inverter: (a) inverter and motor voltages along with load currents, (b) switching cycle view, and (c) enlarged view for a rising voltage transition.

converter, however at the expense of sacrificing the improved harmonic profile and EMI performance of the 3L converter. By splitting the switching transitions of the voltage pulses into two coordinated voltage steps with a brief separation time at the middle voltage level, a Q3L voltage waveform is generated with the advantageous feature of voltage reflection cancellation, where the resultant peak motor voltage can be limited to 20% above the inverter rated voltage. The Q3L T-type converter has a better efficiency compared with the 3L one since the auxiliary switching devices conduct for a significantly shorter time during the Q3L modulation compared with a standard 3L modulation. The effectiveness of the Q3L approach is mainly governed by the accuracy of the dwell time which depends on the cable parameters. Since the cable parameters can slightly vary with the operating temperature, the overvoltage mitigation ability of the Q3L approach can be slightly reduced.

The soft-switching inverters can eliminate the motor terminal overvoltage by increasing the switching rise/fall time of the voltage transitions based on a resonance action between inductive and capacitive elements. As the switching rise/fall time increases, the EMI performance is further improved since the voltage pulses' fronts are smoothly profiled with low dv/dt. Since the switched voltage and current are decoupled, the switching power loss is minimized resulting in an overall efficiency that can be higher than the 2L converter's [21]. Although soft-switching inverters can be implemented in different topologies, they commonly require resonant reactive elements that increase the overall converter size and also require different parametric design depending on the cable length.

V. Conclusion

This paper has evaluated the active control methods that can mitigate the motor terminal overvoltage in SiC-based cable-fed drives. As alternatives to passive filtering techniques, the active control methods, based on using multilevel converters, modifying the PWM scheme, and implementing soft-switching techniques, have the potential to mitigate the reflected voltage phenomenon without significant sacrifice in the overall performance metrics of the SiC-based motor drive system. A qualitative and quantitative comparison between the different active control methods has been presented in this paper, supported with experimental verification.

Acknowledgment

This work was supported in part by the UK EPSRC under grant EP/S00081X/1.

References

[1] A. Morya, M. Moosavi, M. C. Gardner and H. A. Toliyat, "Applications of Wide Bandgap (WBG) devices in AC electric drives: A technology status review," *2017 IEEE International Electric Machines and Drives Conference (IEMDC)*, Miami, FL, 2017, pp. 1-8.

[2] A. K. Morya *et al*., "Wide bandgap devices in AC electric drives: Opportunities and challenges," *IEEE Trans. Transp. Electrific.*, vol. 5, no. 1, pp. 3-20, March 2019.

[3] M. J. Scott *et al*., "Reflected wave phenomenon in motor drive systems using wide bandgap devices," *2014 IEEE Workshop on Wide Bandgap Power Devices and Applications*, Knoxville, TN, 2014, pp. 164-168.

[4] Y. Xu *et al*., "Impact of high switching speed and high switching frequency of wide-bandgap motor drives on electric machines," *IEEE Access*, vol. 9, pp. 82866-82880, 2021.

[5] W. Yin, "Failure mechanism of winding insulations in inverter-fed motors," *IEEE Elect. Insul. Mag.*, vol. 13, no. 6, pp. 18–23, Nov./Dec. 1997.

[6] P. Yi, P. K. S. Murthy and L. Wei, "Performance evaluation of SiC MOSFETs with long power cable and induction motor," *2016 IEEE Energy Conversion Congress and Exposition (ECCE)*, Milwaukee, WI, USA, 2016.

[7] M. S. Diab and X. Yuan, "A modular quasi-multilevel converter using 10kV SiC MOSFETs for medium-voltage cable-fed variable-speed motor drives," in *Proc. IEEE ECCE-Asia'21 Conf*, pp.1-6, May 2021.

[8] B. Narayanasamy, A. S. Sathyanarayanan, F. Luo and C. Chen, "Reflected wave phenomenon in SiC motor drives: Consequences, boundaries, and mitigation," *IEEE Trans. Power Electron.*, vol. 35, no. 10, pp. 10629-10642, Oct. 2020.

[9] J. He, G. Y. Sizov, P. Zhang and N. A. O. Demerdash, "A review of mitigation methods for overvoltage in long-cable-fed PWM AC drives," *2011 IEEE Energy Conversion Congress and Exposition*, Phoenix, AZ, 2011, pp. 2160-2166.

Table I: Assessment of active control methods for overvoltage mitigation

	2L converter	3L T-type converter	Q3L T-type converter	Soft-switched ARCPI
Concept of overvoltage mitigation	-	Reducing the voltage jump of switching transitions	Cancelling the voltage reflections using two coordinated voltage steps	Increasing the switching rise time based on resonance action
Motor peak voltage (at most)	2 pu	1.5 pu	1.2 pu	1 pu
dv/dt **(EMI) at motor side**	V_{dc}/t_r High EMI	$0.5V_{dc}/t_r$ Lower EMI	V_{dc}/t_r High EMI	V_{dc}/t_r Lowest EMI since t_r is longer
Number of switching devices	6 switches	12 switches		
Voltage rating of switching devices	V_{dc}	V_{dc} for main switches and $0.5V_{dc}$ for auxiliary switches		
Passive component count	-	-	-	3 resonant inductors 6 snubber capacitors
Efficiency	Reference	Higher than 2L at high-switching frequencies	Higher than 2L	Higher than 2L
Sensitivity to operating parameters	-	-	The effectiveness is slightly sensitive to cable operating temperature	Different cable lengths may require different resonant parameters

[10] M. Pastura, S. Nuzzo, M. Kohler and D. Barater, "Dv/Dt filtering techniques for electric drives: Review and challenges," *IECON 2019 - 45th Annual Conference of the IEEE Industrial Electronics Society*, Lisbon, Portugal, 2019, pp. 7088-7093.

[11] J. He *et al*., "Multi-domain design optimization of dv/dt filter for SiC-based three-phase inverters in high-frequency motor-drive applications," *IEEE Trans. Ind. Appl.*, vol. 55, no. 5, pp. 5214-5222, Sept.-Oct. 2019.

[12] J. Rodriguez, J.-S. Lai, and F. Z. Peng, "Multilevel inverters: A survey of topologies, controls, and applications," *IEEE Trans. Ind. Electron.*, vol. 49, no. 4, pp. 724–738, Aug. 2002.

[13] F. Endrejat and P. Pillay, "Resonance overvoltages in medium-voltage multilevel drive systems," *IEEE Trans. Ind. Appl.*, vol. 45, no. 4, pp. 1199-1209, July-aug. 2009.

[14] M. Schweizer, I. Lizama, T. Friedli and J. W. Kolar, "Comparison of the chip area usage of 2-level and 3-level voltage source converter topologies," *IECON 2010 - 36th Annual Conference on IEEE Industrial Electronics Society*, Glendale, AZ, 2010.

[15] M. Schweizer and J. W. Kolar, "Design and implementation of a highly efficient three-level T-type converter for low-voltage applications," *IEEE Trans. Power Electron.*, vol. 28, no. 2, pp. 899-907, Feb. 2013.

[16] S. Lee and K. Nam, "An overvoltage suppression scheme for AC motor drives using a half-DC-link voltage level at each PWM transition," *IEEE Trans. Ind. Electron.*, vol. 49, no. 3, pp. 549-557, June 2002.

[17] M. S. Diab and X. Yuan, "A quasi-three-level PWM scheme to combat motor overvoltage in SiC-based single-phase drives," *IEEE Trans. Power Electron.*, vol. 35, no. 12, pp. 12639-12645, Dec. 2020.

[18] M. S. Diab and X. Yuan, "A quasi-three-level modulation scheme to combat motor overvoltage in SiC-based drives with open-end stator winding configurations," *IECON 2020 The 46th Annual Conference of the IEEE Industrial Electronics Society*, Singapore, 2020.

[19] W. Zhou, M. S. Diab and X. Yuan, "Mitigation of motor overvoltage in SiC-device-based drives using a soft-switching inverter," *2020 IEEE Energy Conversion Congress and Exposition (ECCE)*, Detroit, MI, USA, 2020, pp. 662-669.

[20] W. Zhou and X. Yuan, "Experimental evaluation of SiC MOSFETs in comparison to Si IGBTs in a soft-switching converter," *IEEE Trans. Ind. Appl.*, vol. 56, no. 5, pp. 5108-5118, Sept.-Oct. 2020.

[21] B. L. C. Martinez, Rui Li, Ke Ma and Dehong Xu, "Hard switching and soft switching inverters efficiency evaluation," *2008 International Conference on Electrical Machines and Systems*, 2008, pp. 1752-1757.